ORIGINAL ARTICLE

Long non-coding ribonucleic acid ATP2B1-AS1 modulates endothelial permeability through regulating the miR-4729–IQGAP2 axis in diabetic retinopathy

Zengjin Ren, Xue Wang* (iD)

Department of Ophthalmology, The First Affiliated Hospital of Kangda College of Nanjing Medical University, Xuzhou Medical University Affiliated Hospital of Lianyungang, The First People's Hospital of Lianyungang, Jiangsu, China

ABSTRACT

Aims/Introduction: Mounting evidence shows that long non-coding RNAs (lncRNAs) are important to modulate the biological process of diabetic retinopathy (DR). We aimed to investigate the role of lncRNAs in DR and elucidate the exact mechanism.

Materials and Methods: Real-time quantitative polymerase chain reaction was carried out to distinguish the lncRNA ATPase plasma membrane Ca^{2+} transporting 1 antisense RNA 1 (ATP2B1-AS1) expression in DR patients and HG-treated human retinal endothelial cells (HRECs). Dual-luciferase reporter system was used to verify that ATP2B1-AS1 could act as a microRNA (miR)-4729 sponge, and miR-4729 could bind to 3'UTR of IQ motif-containing GTPase-activating protein 2 (IQGAP2). Cell proliferation assay, wound healing migration assay, transwell assay, tube formation assay and immunofluorescence were used to investigate cell proliferation, migration and angiogenesis in HRECs.

Results: The present results showed that ATP2B1-AS1 was downregulated in DR patients and high-glucose-induced HRECs. In gain- and loss-of-function assays, ATP2B1-AS1 overexpression could significantly reduce cell proliferation, migration, angiogenesis and permeability induced by high glucose *in vitro*. Additionally, we carried out dual-luciferase reporter experiments to determine that ATP2B1-AS1 could act as a miR-4729 sponge. ATP2B1-AS1 overexpression could rescue miR-4729 mimics and short hairpin RNA-IQGAP2 induced cell proliferation, migration and angiogenesis in HRECs.

Conclusions: The present study showed that ATP2B1-AS1 acted as a miR-4729 sponge to regulate IQGAP2 reducing high-glucose-induced endothelial dysfunction in DR.

INTRODUCTION

Diabetic retinopathy (DR) is becoming one of the most severe health problems globally, and can cause irreversible visual impairment and blindness[1,2]. DR, a typical diabetes mellitus complication, could be prompted by hyperglycemia. According to the report from the World Health Organization, approximately 422 million people currently suffer from diabetes worldwide, especially in low- or middle-income countries[3]. This population is predicted to increase to account for one in five Americans by 2050. Among diabetes patients, >95 million patients have DR, of which one-third have vision-threatening

DR[4]. A total of 98% of type 1 diabetes patients and 80% of type 2 diabetes patients would develop DR. In addition, the chance of sight-threatening DR is also higher in type 1 diabetes patients[5].

It has been considered that DR is a kind of microvascular disease, whose pathology includes loss of pericytes, microvascular endothelial cells damage and blood–retinal barrier breakdown in the early stage[6,7]. The mechanisms in the DR include oxidative stress, mitochondrial dysfunction, glycation endproducts production and impaired bioenergetics[8–10]. According to microvascular changes, DR has been divided into two stages. One is non-proliferative DR and the other is proliferative DR in the end-stage. Non-proliferative DR is caused by many facts;

for instance, vascular tortuosity, microaneurysms, retinal hemorrhages and white cotton spots[11]. In contrast, proliferative DR results in severe vision impairment, which is featured by aberrant neovascularization, epiretinal membrane, preretinal or vitreous hemorrhages and tractional detachment of the retina[12].

As innovative sequencing technologies are developed and emerge, an increasing number of non-coding loci have been identified and confirmed the function in biological processes[13]. Furthermore, transcription identification grows at an unprecedented speed. Among the various kinds of non-coding ribonucleic acids (RNAs), long non-coding RNAs (lncRNAs) are an important branch of RNA transcripts, whose base numbers are >200 pairs, without protein-coding potential[14]. ATPase plasma membrane Ca^{2+} transporting 1 antisense RNA 1 (ATP2B1-AS1), which is also called long intergenic non-protein-coding RNA 936 (LINC00936), has been confirmed to be important in chronic renal failure-induced renal interstitial fibrosis and myocardial infarction[15,16]. However, the role of ATP2B1-AS1 in DR remains unknown. In the present research, we investigated the function of ATP2B1-AS1 in DR through the regulation of the miR-4729 and IQ motif-containing GTPase-activating protein 2 (IQGAP2), which has been identified as a tumor suppressor in many cancers[17], to control endothelial cells dysfunction. According to the present study, ATP2B1-AS1 could act as a therapeutic target for DR treatment.

MATERIALS AND METHODS

Clinical data
Blood samples were obtained from the First People's Hospital of Lianyungang. All the blood samples were immediately separated and stored at −80°C according to manufacturers. Candidates included 30 type 2 diabetes patients with clinically detected DR. The DR patients' and normal healthy participants' characteristics are listed in Table 1. The study received approval from the First People's Hospital of Lianyungang.

Table 1 | Clinicopathological features of diabetic retinopathy patients ($n = 30$)

Patients	
Age (years)	59.43 ± 7.21
Sex	
Male	22
Female	9
BP (mmHg)	
Systolic	134.38 ± 7.41
Diastolic	79.33 ± 5.96
HbA1c (%)	7.69 ± 0.85
FPG (mg/dL)	7.86 ± 0.65
BMI (kg/m^2)	33.74 ± 3.05

BMI, body mass index; BP, blood pressure; FPG, fasting plasma glucose; HbA1c, glycated hemoglobin.

Animals
The plasmid cloning deoxyribonucleic acid (pcDNA) empty vector and pcDNA lncRNA ATP2B1-AS1 was inserted into the adeno-associated viruses vector plasmid pSNAV1 for viral preparations used for animal transduction. The mice were randomly divided into two groups: adeno-associated viruses-pcDNA and adeno-associated viruses-lncRNA ATP2B1-AS1 groups, and then the diabetes mouse model was induced.

Evans blue staining
Briefly, the mice were anesthetized with isoflurane (CP Pharma, Burgdorf, Germany) and the blood was washed out. Subsequently, Evans blue (Sigma-Aldrich, St. Louis, MO, USA) solution was gently injected into the left ventricle using a syringe. After 30 min of incubation, the dye remaining in the vascular lumen, which did not pass into the aortic wall, and was washed out by injecting 20 mL of phosphate-buffered saline into the left ventricle.

Cell culture
Human retinal endothelial cells (HRECs) and 293T cells were purchased from ScienCell Research Laboratories (San Diego, CA, USA). HRECs were cultured in endothelial cells medium (ScienCell). HRECs were treated with different concentrations of 5 mmol/L glucose and 25 mmol/L glucose (HG). 293T cells were cultured in Dulbecco's modified Eagle's medium (Invitrogen, Carlsbad, CA, USA) supplemented with 10% (v/v) fetal bovine serum (Gibco, Waltham, MA, USA). Cultured cells were maintained at 37°C in a humidified incubator containing 5% CO_2.

Dual luciferase reporter assay
The wild-type (WT) and mutant (MUT) sequences of ATP2B1-AS1 and IQGAP2 were constructed into pmirGLO vectors (Genewiz, Suzhou, China). Cells were each seeded with a proper density in 12-well plates. Then, ATP2B1-AS1-WT/IQGAP2-WT or ATP2B1-AS1-MUT/IQGAP2-MUT were co-transfected with miR-4729 mimic or mimic negative control were transfected into the prepared cells for 24 h. After post-transfection, cells were harvested and the firefly luciferase activity was measured using a dual-luciferase reporter assay system (Promega, Madison, WI, USA).

Cell proliferation assay
The cell proliferative activity was measured by using the Cell Counting Kit-8 (CCK-8) assay (Beyotime, Shanghai, China). All treated cells were seeded into 96-well plates and were starved in a serum-free medium for another 24 h. Cells were incubated with CCK-8 reagent. The absorbance value was detected at 450 nm.

Wound healing migration assay
HRECs were cultured in six-well plates to carry out migration assays. After treatment, a 200-μL pipette tip was used to scratch

to create a linear region void of cell. After 24 h, we used a microscope (Olympus, Tokyo, Japan) to take pictures and measure the width (W) of the scratch wound. The rate of close distance of the wounds was calculated.

Transwell assay

After treatment, cell suspension was added into 24-well transwell chambers with 8-μm pore size filter membrane (Corning Inc., Corning, NY, USA). After 12 h, the medium was removed and cells were fixed with paraformaldehyde. The cells were washed and stained with hematoxylin–eosin. The number of cells was observed and counted under a microscope.

Tube formation assay

The Matrigel (Corning Inc.) was added to a pre-cooled plate. Matrigel was solidified in a humidified 5% CO_2 incubator at 37°C. Then, cells with different treatments were added on Matrigel immediately at a proper density. After 8 h, images were visualized and photographed using a phase contrast inverted microscope.

Western blot analysis

Cells with different treatments were lysed with radioimmuno-precipitation assay buffer (Beyotime). After centrifuge, the BCA Protein Assay Reagent (Beyotime) was used to quantify the protein concentration of lysates. Western blot was carried out in accordance with the standard protocol anywhere. IQGAP2 and actin antibodies were obtained from Cell Signal Technology (Danvers, MA, USA). The bands images were obtained from Image Lab Software (Bio-Rad, Hercules, CA, USA) after adding chemiluminescent substrate (Millipore, Burlington, MA, USA). Image Lab Software was used to analyze results.

Immunofluorescence

Treated cells were cultured on coverslips in confocal plates and fixed using 4% paraformaldehyde (Sigma) treatment for 15 min. The cells were washed with phosphate-buffered saline and permeabilized with 0.3%Triton X. After blocking, cells were incubated with primary antibody VE-cadherin (Abcam, Cambridge, MA, USA) overnight at 4°C. Cells were incubated with secondary antibody and 4′,6-diamidino-2-phenylindole. Images were taken under a microscope.

Real-time reverse transcription quantitative polymerase chain reaction

PrimeScript™ RT reagent Kit (TaKaRa, Shiga, Japan) was used to reverse transcribe complementary deoxyribonucleic acid from total RNA, following the manufacturer's instructions. Quantitative gene expression was carried out using the Roche Light Cycler 480 (Roche, Mannheim, Germany). Relative RNA expression was calculated by the $2^{-\triangle\triangle CT}$ method. Primer sequences were listed below (Genewiz): ATP2B1-AS1, forward: 5′-GGTAAATCGAGGCCCAGAGAT-3, reverse: 5′-ACGTGGATGACAGCGTGTGA-3′; IQGAP2, forward: 5′-AGACCCCGCTATGGCTCTATT-3′, reverse: 5′-GCTTCC TCTAAGTGGCACAGAT-3′; hsa-miR-4729, forward: 5′-TCATTTATCTGTTGGGAAGCTA-3′. 18SrRNA, forward: 5′-CAGCCACCCGAGATTGAGCA-3′, reverse: 5′-TAGTAG CGACGGGCGGTGTG-3′.

Statistical analysis

All statistical analyses were carried out by using SPSS v20.0 (IBM Corp., Armonk, NY, USA). Data are represented as the mean ± standard deviation. Statistical significance between groups was determined using Student's t-test or the one-way ANOVA method. A P-value of <0.05 was considered statistically significant.

RESULTS

ATP2B1-AS1 is downregulated in DR patients and HG-treated HRECs

To identify lncRNAs genes expression in HG-induced HRECs, we carried out gene expression analyses using public microarray GEO datasets (GSE117238). To visualize the expression of lncRNAs profile dataset, we generated a heatmap and volcano plot (Figure 1a,b), and could discriminate the differential lncRNAs expression significantly between low-glucose and high-glucose groups. According to the results, ATP2B1-AS1 was one of the most downregulated genes.

Then, we validated that the expression of ATP2B1-AS1 in HG-treated HRECs was significantly decreased measured by reverse transcription quantitative polymerase chain reaction (RT–qPCR) assay (Figure 1c). The level of ATP2B1-AS1 expression in the plasma, which was obtained from 30 DR patients and 30 normal volunteers, was detected with RT–qPCR. The results showed that ATP2B1-AS1 was decreased in DR patients (Figure 1d). The baseline characteristics of the participants are shown in Table 1.

ATP2B1-AS1 inhibits high-glucose-induced cell proliferation, migration, angiogenesis and permeability

To investigate the function of ATP2B1-AS1, first, we constructed the plasmids of ATP2B1-AS1 and its shRNAs to knockdown its expression in HRECs. RT–qPCR results showed that overexpression and knockdown of ATP2B1-AS1 were feasible (Figure 2a). Then, CCK-8 assay was carried out to show that overexpression of ATP2B1-AS1 could inhibit the proliferation of HRECs significantly, whereas knockdown of ATP2B1-AS1 could promote the cell viability markedly (Figure 2b). Compared with the pcDNA group, ATP2B1-AS1 overexpression significantly decreased the proliferation of HRECs. When treated with HG, the proliferation of HRECs was higher than that in the low-glucose group. (Figure 2c). Overexpression of ATP2B1-AS1 inhibited cell proliferation, which was increased by HG.

The migration ability of HRECs was observed by wound healing migration assay and transwell assay. The migration of HRECs was significantly reduced in the ATP2B1-AS1
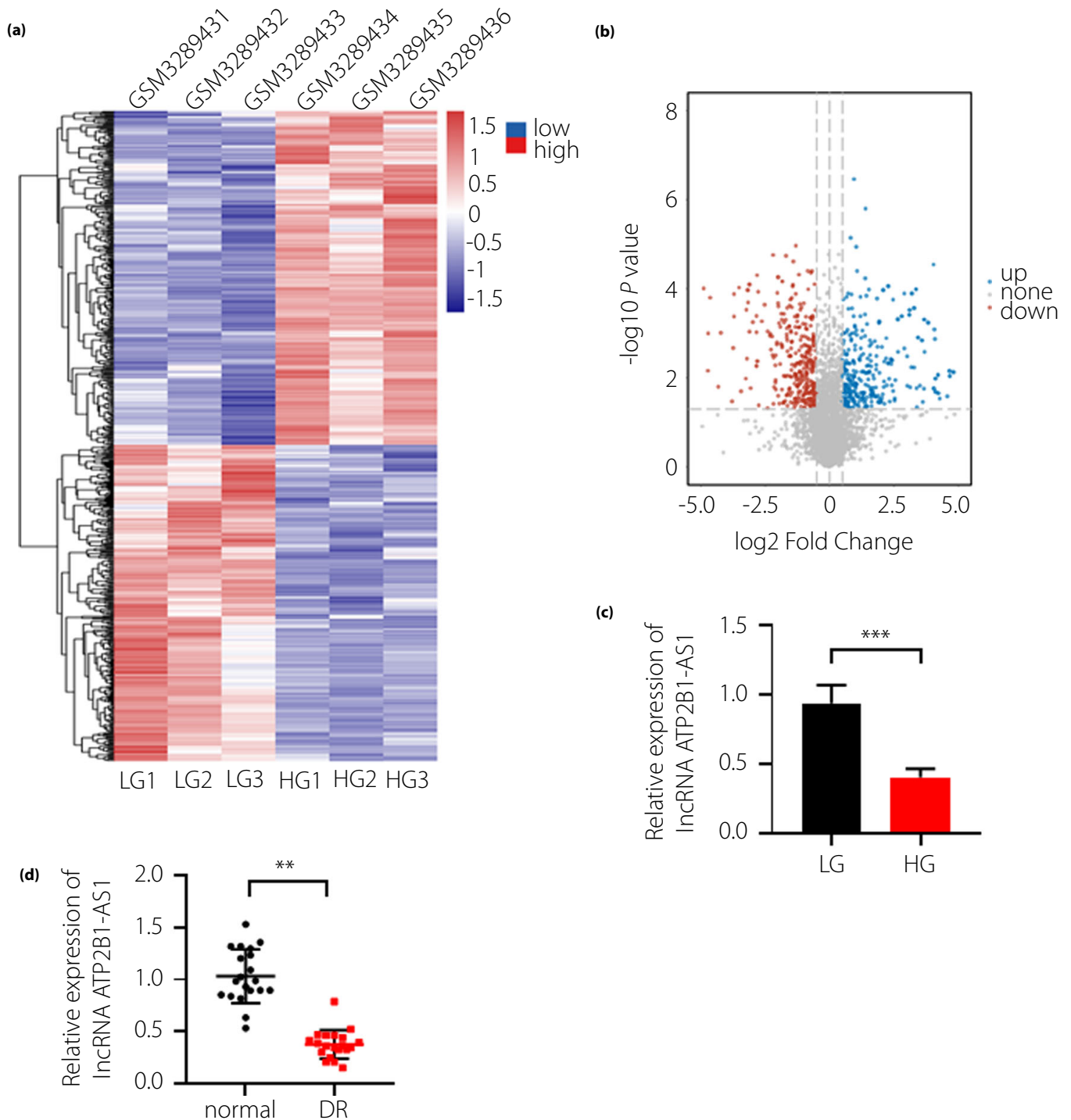
Figure 1 | Identification of ATPase plasma membrane Ca^{2+} transporting 1 antisense ribonucleic acid 1 (ATP2B1-AS1) in diabetic retinopathy (DR) and high-glucose-treated high-glucose-treated human retinal endothelial cells (HRECs). (a) The heatmap of the differentially expressed genes in low glucose (LG) and high glucose (HG). Upregulated genes and downregulated genes are shown in red and blue. (b) Volcano plots showing long non-coding ribonucleic acids expression in the LG and HG groups. The red dots show the significant expressed genes. (c) Reverse transcription quantitative polymerase chain reaction was carried out to detect ATP2B1-AS1 levels in 5 mmol/L or 25 mmol/L glucose treated HRECs. (d) Reverse transcription quantitative polymerase was carried out to distinguish the level of ATP2B1-AS1 in blood samples obtained from DR patients ($n = 30$) and healthy individuals. All values were represented by the mean ± standard deviation. *$P < 0.05$, **$P < 0.01$, ***$P < 0.001$.
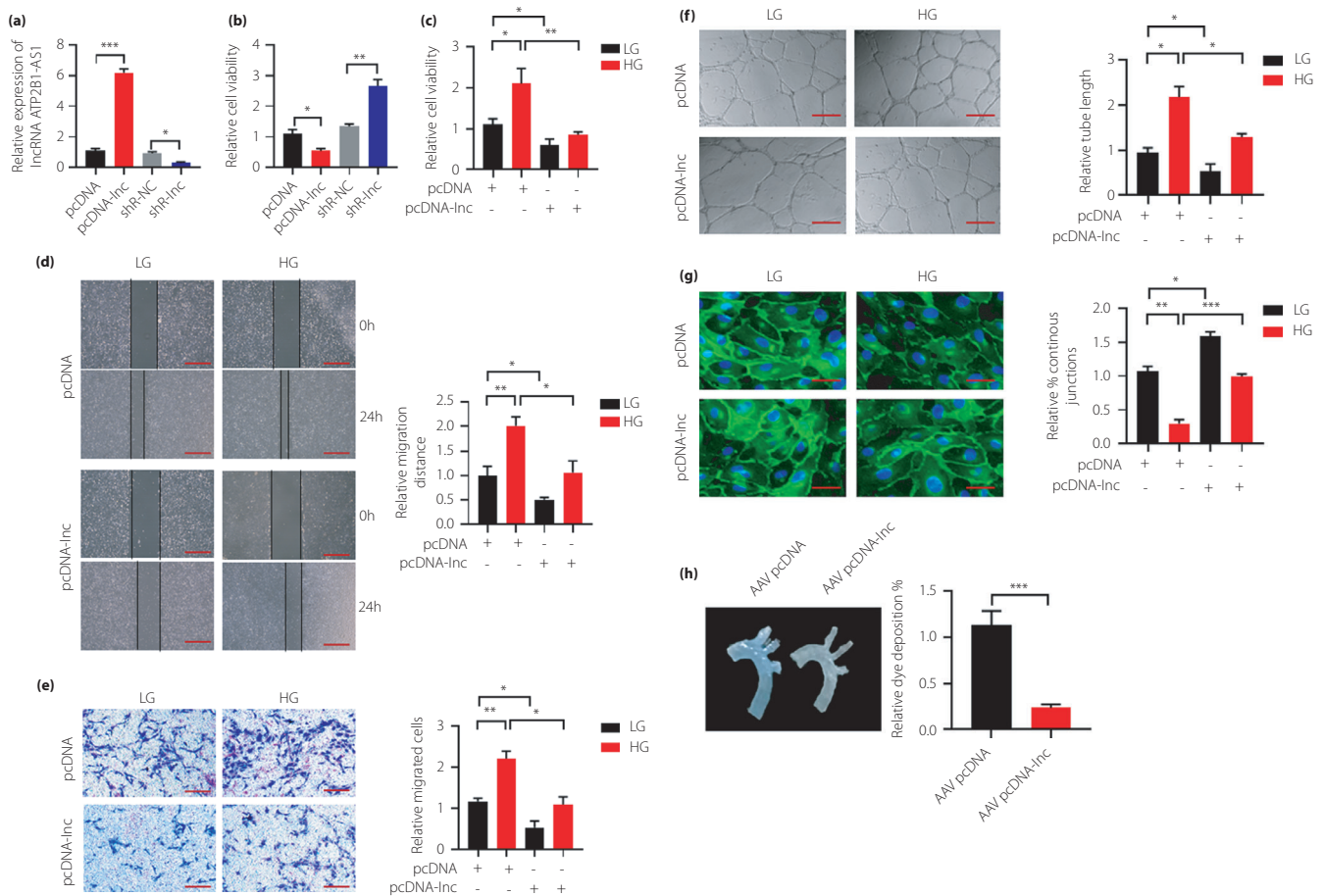
Figure 2 | ATPase plasma membrane Ca^{2+} transporting 1 antisense ribonucleic acid 1 (ATP2B1-AS1) prevents cell proliferation, migration, angiogenesis and permeability. (a) Reverse transcription quantitative polymerase chain reaction was made to measure the expression of ATP2B1-AS1 after transfecting plasmid cloning deoxyribonucleic acid (pcDNA)-long non-coding ribonucleic acids (lncRNA) ATP2B1-AS1 (pcDNA-lnc) and (short hairpin RNA-lncRNA ATP2B1-AS1; shR-lnc) into high-glucose-treated human retinal endothelial cells (HRECs). (b) The level of ATP2B1-AS1 was detected by reverse transcription polymerase chain reaction after transfecting pcDNA-lnc and shR-lnc into HRECs by Cell Counting Kit-8 assay. (c) Proliferation of HRECs was detected by Cell Counting Kit-8 assay. (d, e) Migration ability was measured by wound healing migration assay and transwell assay. (f) Tube formation assay was used to distinguish angiogenesis ability in HRECs. (g) Cell junctional assembly formation of CDH5 staining. (h) Vascular permeability was detected by using evans blue injection. All values were represented by the mean ± standard deviation. *$P < 0.05$, **$P < 0.01$, ***$P < 0.001$.

overexpression group compared with the pcDNA group under 25 mmol/L glucose (Figure 2d,e). To explore whether ATP2B1-AS1 had an impact on angiogenesis, we carried out the tube formation assay and it showed that the number of tubes was increased under the high-glucose condition. As expected, the ATP2B1-AS1 overexpression group showed fewer tube numbers compared with the pcDNA group (Figure 2f). To further investigate whether ATP2B1-AS1 has an effect on cell permeability, immunofluorescence showed that a hyperglycemic HRECs model of DR increased permeability in response to glucose, whereas ATP2B1-AS1 overexpression could reduce cell permeability (Figure 2g). We used adeno-associated viruses to achieve endothelial-specific exogenous expression of lncRNA ATP2B1-AS1 in mice endothelium for 2 weeks, and then

induced the diabetes mice model. We examined vascular permeability by using Evans blue injection. We observed that LncRNA ATP2B1-AS1 overexpression could reduce vascular permeability (Figure 2h). These results showed that ATP2B1-AS1 overexpression negatively regulated cell proliferation, migration and angiogenesis in HG-treated HRECs.

ATP2B1-AS1 serves a sponge to miR-4729

To elucidate whether ATP2B1-AS1 could act as a competing endogenous RNA to regulate gene expression, the MicroRNA Target Prediction Database was carried out to predict the potential microRNA binding sites in ATP2B1-AS1. As shown in Figure 3a, miR-4729 gained the highest score among the entire list of microRNAs. We chose miR-4729 for further

research. The dual-luciferase assay showed that miR-4729 mimics could significantly reduce luciferase activity in the wild-type ATP2B1-AS1 transfected group. However, there was no change in activity of luciferase when transfecting mutant ATP2B1-AS1 (Figure 3b). It suggested that miR-4729 could bind to ATP2B1-AS1. In addition, to verify whether ATP2B1-AS1 takes part in regulating expression of miR-4729, we overexpressed or knocked down ATP2B1-AS1 in HRECs. The RT–qPCR showed that the level of miR-4729 was increased significantly after ATP2B1-AS1 knockdown, and decreased when overexpressing ATP2B1-AS1 in HRECs (Figure 3c). Meanwhile, we detected the level of miR-4729 in between DR patients and healthy people. RT–qPCR indicated that miR-4729 was upregulated in DR patients (Figure 3d). Furthermore, Pearson's correlation analysis was carried out to evaluate the relationship between the expression of miR-4729 and ATP2B1-AS1. The analysis showed that the level of miR-4729 was negatively correlated with ATP2B1-AS1 (Figure 3e).

ATP2B1-AS1 regulates high-glucose-induced cell proliferation, migration, angiogenesis and permeability through miR-4729–IQGAP2 axis

Using the bioinformatics database, IQGAP2 was identified as a probable downstream target of miR-4729. The dual-luciferase assay showed the binding affinity between IQGAP2 and miR-4729. As shown in Figure 4a, miR-4729 reduced luciferase activity and the effect rescued by transfecting mutation. It showed that miR-4729 could bind to IQGAP2. To verify this hypothesis, the ATP2B1-AS1 plasmids and/or miR-4729 mimics were transfected into HRECs. Western blot showed that the ATP2B1-AS1 overexpression significantly increased the expression of IQGAP2, and miR-4729 mimics decreased the level of IQGAP2. miR-4729 mimics could also decrease expression of IQGAP2, despite ATP2B1-AS1 overexpression (Figure 4b). Furthermore, CCK-8 assay showed that the capacity of cell proliferation reduction in the ATP2B1-AS1 overexpression group was upregulated after transfecting miR-4729 mimics or shR-IQGAP2 in HRECs under high-glucose condition (Figure 4c). Additionally, wound healing migration assay and transwell assay showed that the decreased migration ability in ATP2B1-AS1 overexpression was reversed after miR-4729 overexpression and IQGAP2 knockdown (Figure 4d,e). Finally, tube formation assay and immunofluorescence showed that the decreased angiogenesis and permeability after ATP2B1-AS1 overexpression was encouraged by miR-4729 overexpression and IQGAP2 knockdown (Figure 4f,g). Taken together, these data showed that ATP2B1-AS1 might regulate cell proliferation, migration, angiogenesis and permeability through the miR-4729–IQGAP2 axis.
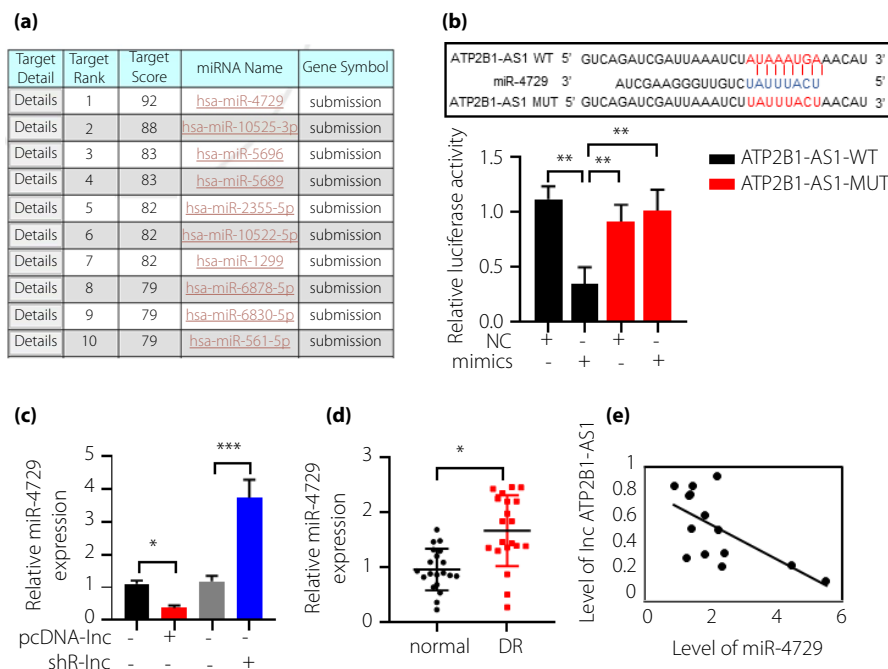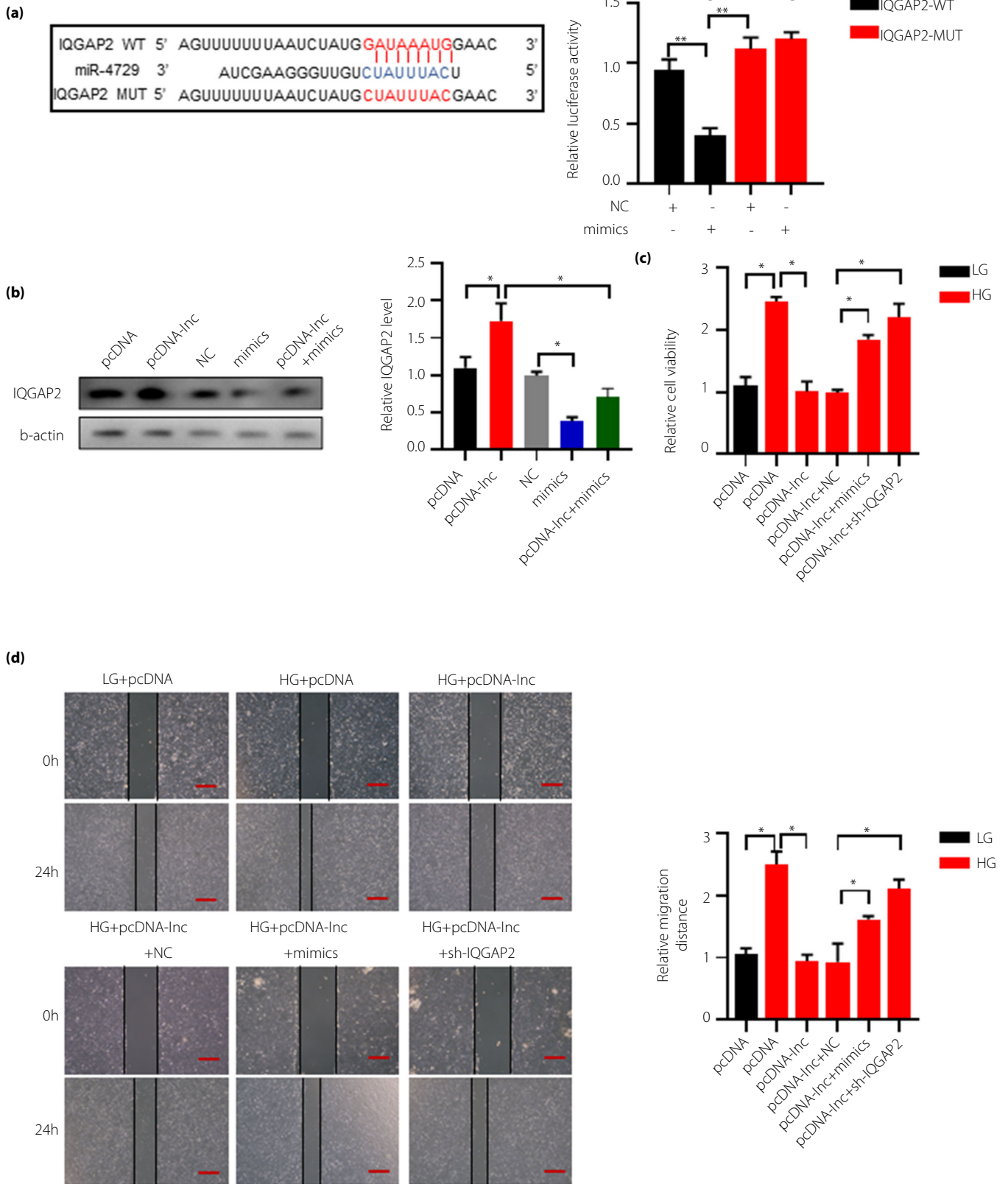

Figure 3 | ATPase plasma membrane Ca^{2+} transporting 1 antisense ribonucleic acid 1 (ATP2B1-AS1) sponges microRNA (miR)-4729. The microRNAs lists and scores on predicted by using the MicroRNA Target Prediction Database. (b) Predicted miR-4729 binding sites in 3'UTR of ATP2B1-AS1 and dual luciferase report assay in ATP2B1-AS1-wild type (WT) or ATP2B1-AS1-mutation (MUT) co-transfected with miR negative control (NC) or miR-4729 mimics. (c) Level of miR-4729 in high-glucose-treated human retinal endothelial cells (HRECs) transfected with shR-lnc or pcDNA-lnc. (d) miR-4729 expression in blood from diabetes retinopathy (DR) patients ($n = 30$) and non-DR individuals. (e) Pearson's correlation analysis was used to check the relationship between ATP2B1-AS1 and miR-4729. All values were represented by the mean ± standard deviation. *$P < 0.05$, **$P < 0.01$, ***$P < 0.001$.

(a)
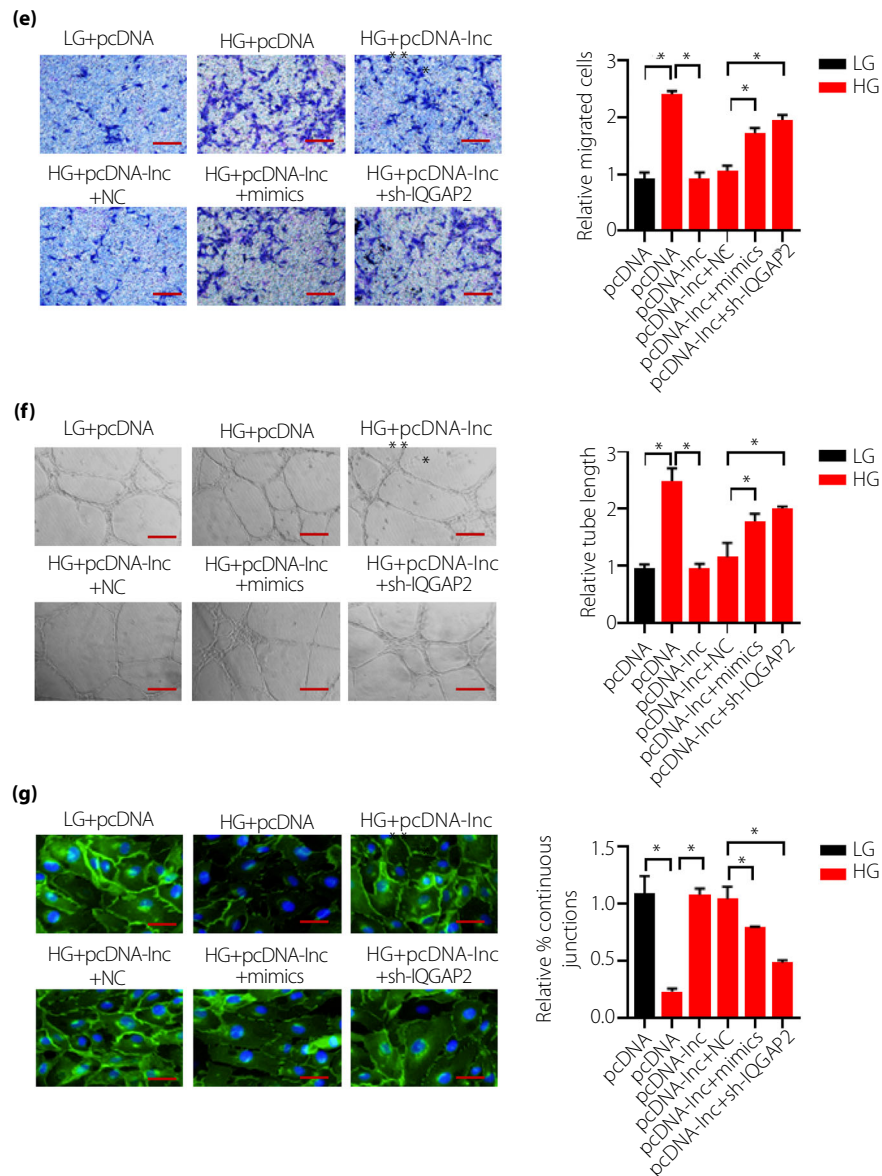

(b)

(c)

(d)

Figure 4 | ATPase plasma membrane Ca^{2+} transporting 1 antisense ribonucleic acid 1 (ATP2B1-AS1) reduced high glucose-treated high-glucose-treated human retinal endothelial cells (HRECs) cell proliferation, migration, angiogenesis and permeability through regulating microRNA (miR)-4729–IQ motif-containing GTPase-activating protein 2 (IQGAP2) axis. (a) Schematic indicating the miR-4729 sites in IQGAP2 and dual luciferase assay in IQGAP2-wild type (WT) or IQGAP2-mutation (MUT) treated HRECs co-transfected with miR-NC or miR-4729 mimics. (b) The protein IQGAP2 level was detected by WB after transfection. (c) HRECs proliferation was detected by Cell Counting Kit-8 assay after transfection. (d, e) Migration ability was measured by wound healing migration assay and transwell assay after transfection. (f) Tube formation assay was used to detect the ability of angiogenesis in HRECs after transfection. (g) Cell junctional assembly formation of VE-cadherin staining after transfection. All values were represented by the mean ± standard deviation. $*P < 0.05$, $**P < 0.01$, $***P < 0.001$.

DISCUSSION

As the most common microvascular complication of diabetes, DR is becoming one of the leading causes of irreversible vision impairment worldwide. There are many vascular manifestations involved in DR progress; for instance, capillary loss, venous beading, microaneurysms, retinal vascular leakage, diabetic macular edema and so on. Ophthalmic examinations can detect vitreous hemorrhage through the transparent cornea[18]. Nowadays, the main DR treatment methods include antivascular endothelial growth factor medications, laser photocoagulation, corticosteroids injections and surgery[19]. These interventions are proven to be effective in vascular proliferation inhibition and diabetic macular edema reduction, resulting in saving eyesight. Unfortunately, the aforementioned measures are limited
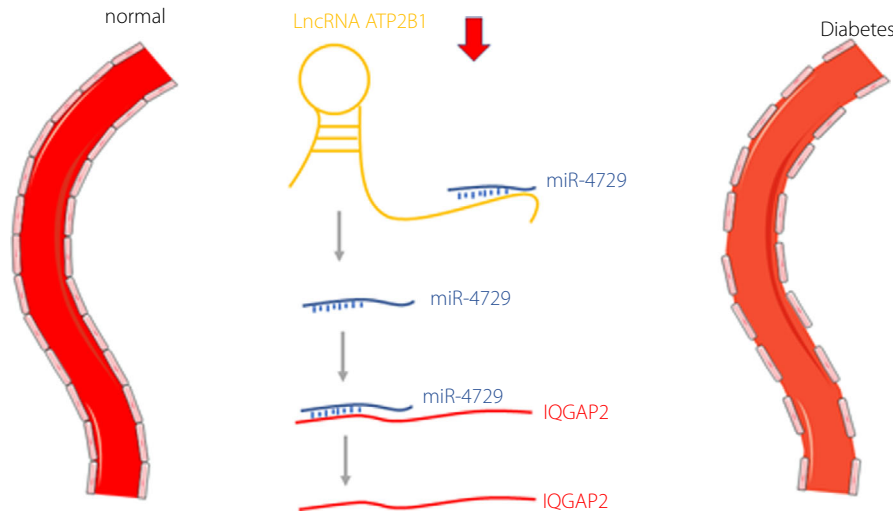
Figure 5 | Graphic model of long non-coding ribonucleic acids (lncRNA) ATPase plasma membrane Ca^{2+} transporting 1 antisense ribonucleic acid 1 (ATP2B1-AS1) modulates endothelial permeability. ATP2B1-AS1 acts as a microRNA (miR)-4729 sponge to regulate IQ motif-containing GTPase-activating protein 2 (IQGAP2) reduce high-glucose-induced endothelial dysfunction in diabetic retinopathy. Decreased ATP2B1-AS1 significantly reduced cell proliferation, migration, angiogenesis and permeability through the miR-4729–IQGAP2 axis in response to hyperglycemia.

because of a short therapeutic half-life, and attendant adverse effects, injection site bleeding and intraocular pressure increase[20,21].

Recently, the potential relevance of lncRNAs dysregulation and DR has attracted much attention[22]. The researchers showed that the mitogen-activated protein kinase signaling pathway might be involved in metastasis-associated lung adenocarcinoma transcript 1 function to amplify the proliferation of RF/6A cells under hyperglycemic circumstances[23]. Zhang *et al.*[24] reported that there is the same intricate mechanistic relationship between nuclear factor-κB and myocardial infarction-associated transcript under hyperglycemic stress. Nuclear factor-κB has indeed been shown to selectively recruit to the myocardial infarction-associated transcript promoter, which can be subsequently heightened under the stimulation of high glucose in primary rat retinal Müller cells[24]. The overexpression of H19 in HG-treated HRECs significantly inhibited the effect caused by high glucose, showing a protective role of H19 in DR[25]. Here, we identified a new lncRNA, ATP2B1-AS1, and examined whether ATP2B1-AS1 can regulate proliferation of HRECs treated with normal glucose. Unsurprisingly, ATP2B1-AS1 regulated cell proliferation in HRECs. Furthermore, ATP2B1-AS1 dramatically reversed the trends under hyperglycemia, in which increased cell proliferation, migration and tube formation were shown. According to this evidence, we reported it was involved in retinal angiogenesis under high-glucose conditions. Furthermore, the exact mechanism that lncRNAs sponge microRNAs to regulate gene expression has still been uncovered. It is the same that ATP2B1-AS1 can interact with microRNAs directly. According to the MicroRNA Target Prediction Database, miR-4729 gained the highest score among the entire list of microRNAs. Thus, we hypothesized

that ATP2B1-AS1 acted as a miR-4729 sponge, efficiently reversing the inhibitory effect by ATP2B1-AS1 knockdown. Furthermore, upregulation of miR-4729 was also significantly decreased by ATP2B1-AS1 overexpression.

With respect to IQ motif-containing GTPase-activating protein 2 (IQGAP2), it functions as a scaffolding protein that regulates the cytoskeleton by juxtaposing Rho GTPase and Ca^{2+}/calmodulin signals[26]. Low expression of IQGAP2 has been identified in ovarian cancer, prostate cancer, hepatocellular carcinoma and gastric cancer[27–30], suggesting that IQGAP2 functions as a tumor suppressor. However, the IQGAP2 biological functions in DR are yet to be uncovered. Herein, we predicted and confirmed that miR-4729 can bind to the 3′UTR of IQGAP2, reducing expression of IQGAP2 in retinal endothelial cells. It is important to note that the expression of IQGAP2 was post-transcriptionally regulated by ATP2B1-AS1 through miR-4729 in HG-treated HRECs.

In a summary, the present study uncovered for the first time that ATP2B1-AS1 was decreased in DR progression. Overexpressing ATP2B1-AS1 significantly reduced cell proliferation, migration, angiogenesis and permeability in response to hyperglycemia. Markedly, all effects regulated by ATP2B1-AS1 were through the miR-4729–IQGAP2 axis (Figure 5). In a conclusion, the present study showed the function of ATP2B1-AS1 in DR, and the promising value of the ATP2B1-AS1–miR-4729–IQGAP2 axis to treat DR.

DISCLOSURE

The authors declare no conflict of interest.

Approval of the research protocol: N/A.

Informed consent: N/A.

Approval date of registry was 7 November 2017 and the registration no. of the study/trial: No.KY-2017325.

Animal studies: N/A.

REFERENCES

1. Bourne R, Steinmetz J, Flaxman S, et al. Trends in prevalence of blindness and distance and near vision impairment over 30 years: an analysis for the global burden of disease study. *Lancet Glob Health* 2021; 9: e130–e143.

2. Li BY, Tan W, Zou JL, et al. Role of interferons in diabetic retinopathy. *World J Diabetes* 2021; 12: 939–953.

3. Hristova E, Koseva D, Zlatarova Z, et al. Diabetic retinopathy screening and registration in Europe-narrative review. *Healthcare* 2021; 9: 745.

4. Lee R, Wong TY, Sabanayagam C. Epidemiology of diabetic retinopathy, diabetic macular edema and related vision loss. *Eye Vis* 2015; 2: 17.

5. Thomas RL, Dunstan FD, Luzio SD, et al. Prevalence of diabetic retinopathy within a national diabetic retinopathy screening service. *Br J Ophthalmol* 2015; 99: 64–68.

6. Beltramo E, Porta M. Pericyte loss in diabetic retinopathy: mechanisms and consequences. *Curr Med Chem* 2013; 20: 3218–3225.

7. Mrugacz M, Bryl A, Zorena K. Retinal vascular endothelial cell dysfunction and neuroretinal degeneration in diabetic patients. *J Clin Med* 2021; 10: 458.

8. Dong XX, Wang Y, Qin ZH. Molecular mechanisms of excitotoxicity and their relevance to pathogenesis of neurodegenerative diseases. *Acta Pharmacol Sin* 2009; 30: 379–387.

9. Jellinger KA. Should the word 'dementia' be forgotten? *J Cell Mol Med* 2010; 14: 2415–2416.

10. Rosa MD, Distefano G, Gagliano C, et al. Autophagy in diabetic retinopathy. *Curr Neuropharmacol* 2016; 14: 810–825.

11. Karst SG, Lammer J, Radwan SH, et al. Characterization of in vivo retinal lesions of diabetic retinopathy using adaptive optics scanning laser ophthalmoscopy. *Int J Endocrinol* 2018; 2018: 7492946.

12. Gotzaridis EV, Lit ES, D'Amico DJ. Progress in vitreoretinal surgery for proliferative diabetic retinopathy. *Semin Ophthalmol* 2001; 16: 31–40.

13. Gloss BS, Dinger ME. Realizing the significance of noncoding functionality in clinical genomics. *Exp Mol Med* 2018; 50: 1–8.

14. Kino T, Hurt DE, Ichijo T, et al. Noncoding RNA gas5 is a growth arrest- and starvation-associated repressor of the glucocorticoid receptor. *Sci Signal* 2010; 3: ra8.

15. Song KY, Zhang XZ, Li F, et al. Silencing of ATP2b1-AS1 contributes to protection against myocardial infarction in mouse via blocking NFKBIA-mediated NF-kappab signalling pathway. *J Cell Mol Med* 2020; 24: 4466–4479.

16. Chen W, Zhang L, Zhou ZQ, et al. Effects of long non-coding RNA LINC00963 on renal interstitial fibrosis and oxidative stress of rats with chronic renal failure via the foxo signaling pathway. *Cell Physiol Biochem* 2018; 46: 815–828.

17. Hedman AC, Smith JM, Sacks DB. The biology of IQGAP proteins: beyond the cytoskeleton. *EMBO Rep* 2015; 16: 427–446.

18. Ceravolo I, Oliverio GW, Alibrandi A, et al. The application of structural retinal biomarkers to evaluate the effect of intravitreal ranibizumab and dexamethasone intravitreal implant on treatment of diabetic macular Edema. *Diagnostics* 2020; 10: 413.

19. Singer MA, Kermany DS, Waters J, et al. Diabetic macular edema: it is more than just VEGF. *F1000Research* 2016; 5: 1019

20. Gote V, Sikder S, Sicotte J, et al. Ocular drug delivery: present innovations and future challenges. *J Pharmacol Exp Ther* 2019; 370: 602–624.

21. Joseph RR, Venkatraman SS. Drug delivery to the eye: what benefits do nanocarriers offer? *Nanomedicine* 2017; 12: 683–702.

22. Biswas S, Sarabusky M, Chakrabarti S. Diabetic retinopathy, lncRNAs, and inflammation: a dynamic, interconnected network. *J Clin Med* 2019; 8.

23. Yan B, Tao ZF, Li XM, et al. Aberrant expression of long noncoding RNAs in early diabetic retinopathy. *Investig Ophthalmol Vis Sci* 2014; 55: 941–951.

24. Zhang J, Chen M, Chen J, et al. Long non-coding RNA MIAT acts as a biomarker in diabetic retinopathy by absorbing mir-29b and regulating cell apoptosis. *Biosci Rep* 2017; 37.

25. Thomas AA, Biswas S, Feng B, et al. LncRNA H19 prevents endothelial-mesenchymal transition in diabetic retinopathy. *Diabetologia* 2019; 62: 517–530.

26. Ghaleb AM, Bialkowska AB, Snider AJ, et al. IQ Motif-containing GTPase-activating protein 2 (IQGAP2) is a novel regulator of colonic inflammation in mice. *PLoS One* 2015; 10: e0129314.

27. Gnatenko DV, Xu X, Zhu W, et al. Transcript profiling identifies iqgap2(-/-) mouse as a model for advanced human hepatocellular carcinoma. *PLoS One* 2013; 8: e71826.

28. Tang T, Wang J, Zhang L, et al. IQGAP2 acts as an independent prognostic factor and is related to immunosuppression in DLBCL. *BMC Cancer* 2021; 21: 603.

29. Deng Z, Wang L, Hou H, et al. Epigenetic regulation of iqgap2 promotes ovarian cancer progression via activating Wnt/beta-catenin signaling. *Int J Oncol* 2016; 48: 153–160.

30. Xu L, Shao Y, Ren L, et al. IQGAP2 inhibits migration and invasion of gastric cancer cells via elevating SHIP2 phosphatase activity. *Int J Mol Sci* 2020; 21: 1968.